

## Heterogeneity in Classical and Non-Classical Nucleation

Natali Gulbahce

Clark University, Department of Physics, Worcester, MA 01610 and  
Los Alamos National Laboratory, CCS-3, MS-B256, Los Alamos, NM 87545

W. K. Klein

Boston University, Department of Physics, Boston, MA 02215 and  
Los Alamos National Laboratory, T-DO, Los Alamos, NM 87545

Harvey Gould

Clark University, Department of Physics, Worcester, MA 01610  
(Dated: April 14, 2024)

We investigate heterogeneous and homogeneous nucleation in nearest-neighbor and long-range Ising models for various quench depths. We find that the system has a true crossover from heterogeneous to homogeneous nucleation for increasing quench depth only if the interaction is sufficiently long-range. The survival curves, defined as the fraction of systems that remain in the metastable state after a given time, have qualitatively different shapes as a function of quench depth for heterogeneous and homogeneous nucleation when the interaction is short-range, but have identical shapes within the accuracy of our data for long-range interactions.

Nucleation, the process by which a metastable state decays, plays an essential role in a wide variety of systems. The nucleation mechanism involves the appearance of a critical droplet which overcomes a free energy barrier and initiates a decay into the stable state. In homogeneous nucleation the droplet forms due to spontaneous fluctuations. Heterogeneous nucleation occurs when the droplet forms with the help of a wall, defect, or an impurity such as an aerosol. Both homogeneous and heterogeneous nucleation are technologically important, but much greater progress has been made in understanding homogeneous nucleation [1, 2, 3, 4] than heterogeneous nucleation [5, 6, 7, 8, 9].

Existing theories of heterogeneous nucleation are phenomenological and assume that the homogeneous theory can be adapted to the heterogeneous case [5, 6, 7, 10]. The predictions of these theories have been compared to experiment, but the comparisons have been indirect by necessity, and the phenomenological nature of the theories makes the connection to experiment tenuous.

The existing theories of heterogeneous nucleation assume that the homogeneous nucleation process is classical, that is, the droplet is assumed to have a distinct volume and surface and the structure of the droplet interior is the same as the stable phase [5, 6, 7]. No theoretical or numerical studies have been undertaken of the effect of impurities on nucleation near the pseudospinodal [11, 12], where in the homogeneous case the droplets are diffuse with no sharp surface/volume distinction [3, 13]. This lack is an important omission because many systems such as metals [14] and polymers [15] have a long-range/near-mean-field nature with important pseudospinodal effects. We will find that heterogeneous nucleation in near-mean-field systems with long-range interactions differs in important respects from heterogeneous nucleation in sys-

tems for which homogeneous nucleation is classical.

In this letter we discuss our simulations of the effect of an isolated impurity and a wall on nucleation. The simulations were done on  $d = 2$  Ising models at temperature  $T = 4T_c = 9$  with an applied magnetic field of magnitude  $h$ . We used the Metropolis algorithm for about 100 Monte Carlo steps per spin (mcs) to equilibrate the system and then reversed the field. The magnetization of the stable phase is negative. As we will discuss, the system generally remains in a metastable state for some time before the transition to the stable phase. We simulated systems with interaction range  $R = 1$  (nearest neighbor) and  $R = 10$  with linear dimension  $L = 100$  (unless otherwise stated), and  $R = 20$  with  $L = 200$ . The isolated impurity consists of 5 spins in the shape of a + sign, fixed in the direction of the stable phase. The effect of the impurity on the nucleation rate, the probability of heterogeneous and homogeneous nucleation as a function of quench depth  $h$ , and the structure of the critical droplet was studied.

In Table I we show  $f_{\text{impurity}}$ , the fraction of droplets that form on the isolated impurity, and  $f_{\text{other}}$ , the fraction of droplets that form on non-impurity sites, even though an impurity is present. The number of trials was in the range of 100 to 1000. For both  $R = 1$  and  $R = 10$  and shallow quenches, that is, close to the  $h = 0$  coexistence curve, the droplet forms on the impurity in all of our trials. Because the nucleation process is stochastic, we expect that a few droplets would nucleate on non-impurity sites if we do significantly more trials. As  $h$  is increased, more droplets form on non-impurity sites. This result was found for short-range systems using a phase field model [7].

However, there is a significant qualitative difference for deeper quenches between the  $R = 1$  and  $R = 10$  systems.

To see this difference, we plot in Fig. 1 the magnetization per spin  $m$  as a function of time for values of  $h$  where the fraction of droplet formation events on non-purity spins becomes significant. For  $R = 10$  there is a distinct plateau where  $m$  remains roughly constant. This plateau is associated with the metastable state. However, for  $R = 1$  there is no plateau at this quench depth, and thus the system is not in a metastable state.

TABLE I: The fraction of droplet formation events at spins away from the impurity,  $f_{\text{other}}$ , and on the impurity,  $f_{\text{impurity}}$ , for  $R = 1$  and  $R = 10$  as a function of the quench depth  $h$  for  $L = 240$ . As shown in Fig. 1, the droplet formation events for deeper quenches correspond to nucleation only for  $R = 10$ .

R = 1			R = 10		
h	$f_{\text{other}}$	$f_{\text{impurity}}$	h	$f_{\text{other}}$	$f_{\text{impurity}}$
0.25	0.0	1.0	1.12	0.07	0.93
0.30	0.0	1.0	1.13	0.14	0.86
0.35	0.0	1.0	1.14	0.13	0.87
0.40	0.03	0.97	1.15	0.21	0.79
0.45	0.02	0.98	1.16	0.32	0.68

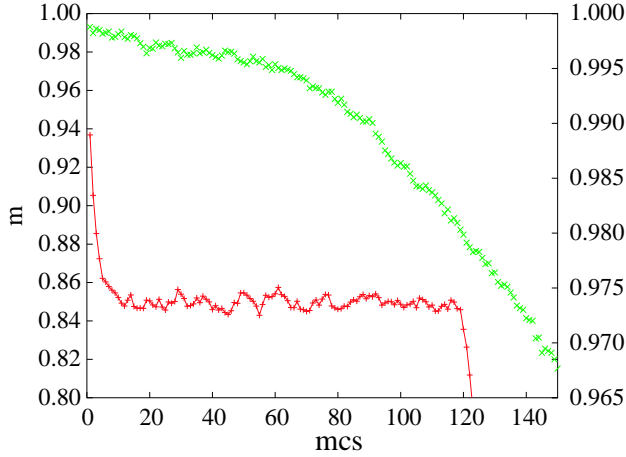


FIG. 1: (color online) The magnetization per spin  $m$  as a function of time (mcs) for  $R = 1$  at  $h = 0.40$  (x) (right axis) and  $R = 10$  at  $h = 1.15$  (+) (left axis). Note the flat region of  $m$  where the  $R = 10$  system is in metastable equilibrium. There is no metastable equilibrium for  $R = 1$  and  $h = 0.40$ .

In nucleation a critical droplet is a saddle point object, which implies that it has an equal probability of growing to the stable state or shrinking back to the metastable state if the system is perturbed at the time of nucleation [1, 2, 3]. We first ran the simulation until a droplet formed and the system proceeded to the stable state. The spin configurations and the current state of the random number generator were saved at various times. We then chose an intervention time at which the critical droplet might have appeared, made 20 copies of the system, and restarted the runs with a different random number seed

for each copy [16]. If the intervention time corresponds to the formation of a saddle point object, one half of the copies will go to the stable phase at approximately the same time and place as in the original run and one half will return to the metastable state. If greater than one half return to the metastable state, the intervention time is too early. If greater than one half proceed to the stable phase, the intervention time is in the growth phase. Although there will be significant fluctuations with 20 trials, this number of trials is sufficient for our purpose.

TABLE II: The number  $n$  of interventions (out of 20) for which the system goes into the stable phase at approximately the same time and place as in the original run;  $t$  corresponds to the intervention time when the random number seed was changed. (The term "no impurity" signifies that no impurity was present in the system.)

	$t$ (mcs)				
	$n$				
R = 1 (no impurity)	140	148	151	155	160
h = 0:6	1	5	11	17	20
R = 1 (with impurity)	70	90	150	250	500
h = 0:4	10	5	15	10	20
R = 10 (no impurity)	108	109	110	111	112
h = 1:2	1	8	10	19	20
R = 10 (with impurity)	198	199	200	201	202
h = 1:16	3	5	15	19	20

In Table II we give the number of interventions that proceeded to the stable phase at approximately the same time and place as in the original run. Note that a saddle point structure is found for the homogeneous and heterogeneous critical droplets in the deeper quenches for  $R = 10$ . That is, the fraction of interventions that go to the stable phase is an increasing function of the time of intervention. Similar behavior was found for both values of  $R$  for shallow quenches, with and without the presence of an impurity (data not shown). However, for  $R = 1$  in the presence of an impurity and quench depths deep enough so that we begin to see a non-zero probability of droplet formation at non-purity sites, no saddle point structure is found. In this case the fraction of droplets that proceed to the stable phase at the same time decreases and then increases as the intervention time increases, in contrast to the behavior found for  $R = 10$  and for  $R = 1$  in the absence of an impurity. The lack of a saddle point object for  $R = 1$  and deep quenches is consistent with the fact that no plateau was found in Fig. 1. We conclude that the crossover to a significant probability of homogeneous nucleation as the quench depth increases is found in long-range interaction systems for which the nucleation is not classical [3]. However, in short-range systems the "crossover" occurs at quench depths for which the system is no longer metastable and the decay process cannot be considered to be nucleation [15].

Another quantity of interest is the survival curve, which we define as the fraction of systems that remain in the metastable state after a given time [8, 9]. We perform this measurement in a slightly different but equivalent way to that of Heneghan et al. [8]. We prepare 1000 systems with the same initial condition, but with different random number seeds, and then measure the fraction of systems,  $\langle s \rangle$ , that are in a metastable state for a given value of  $h$  after  $10^4$  Monte Carlo steps per spin.

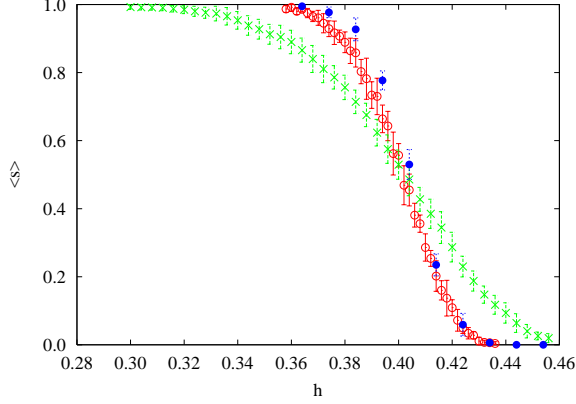


FIG. 2: (color online) Survival curves for heterogeneous nucleation (x), homogeneous nucleation (no impurity present) (o), and heterogeneous nucleation on a wall (o) for  $R = 1$ . The curves for nucleation in the presence of the impurity and on the wall are shifted to the right by  $h = 0.0174$  and  $h = 0.0255$ , respectively, to make it clearer that their shape is qualitatively different from the homogeneous nucleation curve.

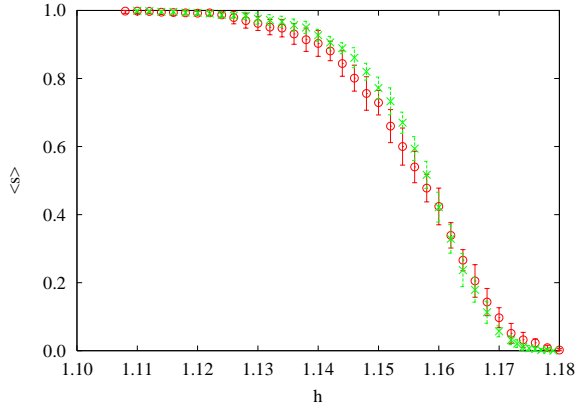


FIG. 3: (color online) Survival curves for homogeneous nucleation (o) (no impurity) and heterogeneous nucleation (x) for  $R = 10$ . The latter curve is shifted to the right by  $h = 0.026$  to make it clearer that the shape of the two curves is almost identical.

In Figs. 2 and 3 we plot the survival curves for  $R = 1$  and  $R = 10$ , respectively. Note that for  $R = 1$  the shape of the survival curves for heterogeneous nucleation on an impurity and on a wall is qualitatively different from

homogeneous nucleation (no impurity present). The wall was implemented with periodic boundary conditions in one direction and open boundaries in the other, and a row of fixed spins at  $x = 0$ . In contrast, for  $R = 10$ , the shape of the survival curves for homogeneous and heterogeneous nucleation is very similar (see Fig. 3).

In Fig. 4 the survival curves for  $R = 10$  for homogeneous nucleation (no impurity present) and nucleation on a wall are shown. The curves have been shifted to lay on top of each other and are almost identical. The results in Figs. 3 and 4 imply that homogeneous nucleation, nucleation on a wall, and nucleation on an isolated impurity have survival curves with similar shapes for long-range interactions. This behavior is reminiscent of the experimental result in Ref. [8] where the survival curves for water nucleating on a wall or on a small crystal of AgI have similar shapes. The survival curves for  $R = 20$  are similar to our results for  $R = 10$  (see Fig. 5). We also did simulations without fixed spins at  $x = 0$  and obtained results similar to our other implementation of a wall (data not shown).

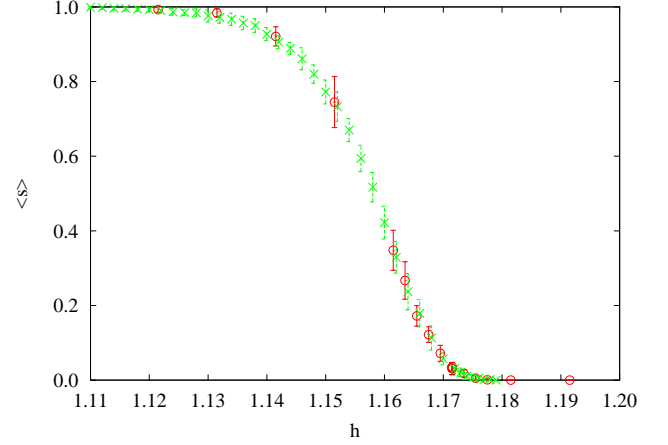


FIG. 4: (color online) Survival curves for homogeneous nucleation (o) and heterogeneous nucleation (x) on a wall for  $R = 10$ . The heterogeneous curve is shifted to the right by  $h = 0.064$ .

For  $R = 1$  and shallow quenches where the nucleation is classical, Fletcher [5] showed theoretically that the radius of the critical droplet was the same for heterogeneous and homogeneous nucleation. Because the droplet interior in classical nucleation is the same as the stable phase, the critical droplets have the same structure aside from the impurity. However, for  $R = 10$ , nucleation takes place near the pseudospinodal [11, 12], and the critical droplets have a diffuse structure [3, 16]. The question arises as to possible changes in the internal structure due to the impurity. In Fig. 6 we plot the density profiles of the critical droplets that form on and away from the impurity for  $R = 10$ . Within the accuracy of our data, the structure appears to be the same.

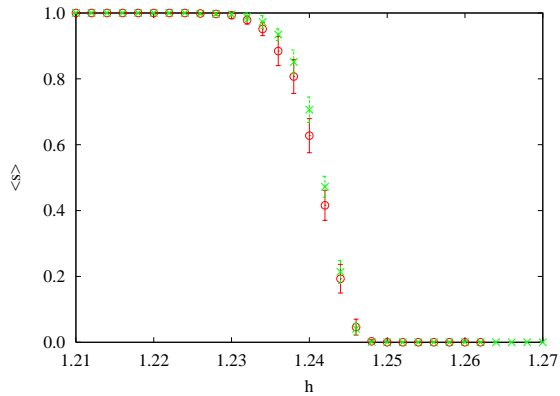


FIG. 5: (color online) The survival curves for homogeneous (no impurity present) (○) and heterogeneous nucleation (×) for  $R = 20$ . The heterogeneous curve is shifted to the right by  $h = 0.006$  to make it clearer that the two curves have similar shapes.

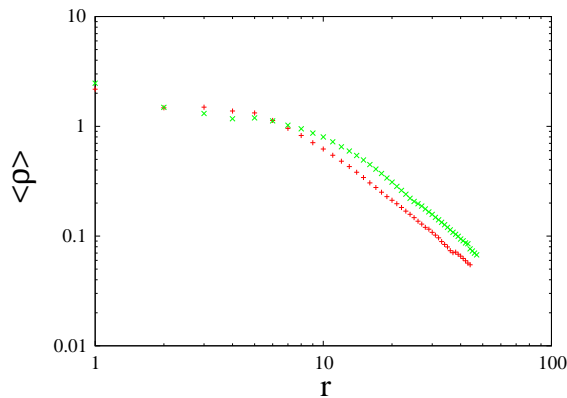


FIG. 6: (color online) The average density  $\langle \rho \rangle$  of the critical droplet as a function of the radius  $r$  measured from the center of mass for  $R = 10$ . (+ signs indicate heterogeneous nucleation and × signs indicate homogeneous nucleation.)

We now summarize our results and discuss their significance. First, heterogeneous nucleation droplets appear to be saddle point objects, which implies that over a significant range of quench depths, simple modifications of homogeneous nucleation theory is possible. Second, the common wisdom [6, 7] that there is a significant crossover from heterogeneous to homogeneous nucleation with increasing quench depth appears to be partially correct. For  $R = 10$  there is a true crossover because the system is still in the metastable state, whereas for  $R = 1$  the “crossover” occurs only after the system has been quenched beyond the metastable state. The existence of a crossover is important for the theoretical treatment of nucleation in systems such as metals where there are long-range interactions [14] and the presence of defects can be important.

We found that the survival curves in long-range systems have the same shape for both homogeneous and

heterogeneous nucleation. This behavior is similar to the results found experimentally in water [8]. However, the survival curve shapes for homogeneous and heterogeneous nucleation are not the same for  $R = 1$ .

The connection between the survival curve shape and the interaction range is very difficult to make experimentally because the latter usually cannot be varied systematically. This connection gives us the first experimentally accessible marker for when a system exhibits nucleation characteristics associated with long-range interactions [3, 13, 16]. That is, if the survival curves have the same shape for homogeneous and heterogeneous nucleation, near-mean-field effects appear to be important.

We also found that the density profile of the critical droplets for heterogeneous and homogeneous nucleation is the same within the accuracy of our data for  $R = 10$  and that heterogeneous nucleation is a saddle point process in the systems we studied and hence can be described by a modified version of homogeneous nucleation. These results are significant for the calculation of nucleation rates and will be discussed in a future publication.

We acknowledge useful conversations with A. D. J. Haymet, Greg Johnson, and Frank Alexander. This work was done at Los Alamos National Laboratory (LA-UR 04-4271). N. Gulbahce acknowledges support from the U.S. Department of Energy under the DOE/BES Program in the Applied Mathematical Sciences, Contract KC-07-01-01 at LANL. W. Klein acknowledges support from the ASC Modeling Program at LANL.

- 
- [1] J. W. Cahn and J. E. Hilliard, *J. Chem. Phys.* **28**, 258 (1958); *ibid.* **31**, 688 (1959).
  - [2] J. S. Langer, *Ann. Phys. (NY)* **41**, 108 (1967).
  - [3] C. Unger and W. Klein, *Phys. Rev. B* **29**, 2698 (1984).
  - [4] D. Kashchiev, *Nucleation: Basic Theory with Applications* (Butterworth-Heinemann, Oxford, 2000).
  - [5] N. H. Fletcher, *J. Chem. Phys.* **29**, 572 (1958).
  - [6] X. Y. Liu, *J. Chem. Phys.* **112**, 9949 (2000).
  - [7] M. Castro, *Phys. Rev. B* **67**, 035412 (2003).
  - [8] A. F. Heneghan, P. W. Wilson, and A. D. J. Haymet, *Proc. Natl. Acad. Sci. USA* **99**, 9631 (2002).
  - [9] A. F. Heneghan, H. Justin Moore, T. Randall Lee, and A. D. J. Haymet, *Chem. Phys. Lett.* **385**, 441 (2004).
  - [10] M. C. Weinberg, *J. Non-Cryst. Solids* **255**, 1 (1999).
  - [11] D. W. Heermann, W. Klein, and D. Stauffer, *Phys. Rev. Lett.* **49**, 1262 (1982).
  - [12] N. Gulbahce, H. Gould, and W. Klein, *Phys. Rev. E* **69**, 036119 (2004).
  - [13] W. Klein and F. Leyvraz, *Phys. Rev. Lett.* **57**, 2845 (1986).
  - [14] W. Klein, T. Lookman, A. Saxena, and D. Hatch, *Phys. Rev. Lett.* **88**, 05701 (2002).
  - [15] K. Binder, *Phys. Rev. A* **29**, 341 (1984).
  - [16] L. Monette and W. Klein, *Phys. Rev. Lett.* **68**, 2326 (1992).